

SEASONAL SNOW COVER MONITORING USING FMCW RADAR

H. Gubler and P. Weilenmann
 Swiss Federal Institute for Snow and Avalanche Research
 CH7260 Weissfluhjoch/Davos

Stationary, ground-buried and mobile, sledge mounted FMCW radars have been used for five years to investigate snow stratigraphy. The systems have proved their feasibility for localized, nondestructive measurements of the development of snow layering, waterequivalence, initial percolation of meltwater, flow depth of dense flow avalanches, and slope perpendicular flow speed profiles. Mobile radars are used to determine areal distributions of snow stratigraphy and waterequivalence.

INTRODUCTION

The method of monitoring snowpack stratigraphy, waterequivalence and wetness using FMCW radars has been investigated experimentally and theoretically in different papers by Ellerbruch and Boyne (1980), Schmidt, Gubler and Hiller (1984) and Gubler and Hiller (1984). The object of this paper is to add recent applications and results.

Eight FMCW (Frequency Modulated Continuous Wave) radars are in use at SFISAR for different investigations: six localized radars buried in the ground, looking upward into the snowcover, at four locations, and two sledge mounted systems looking downward. Two of the radars (X-band and C-band) are installed in the study plot of the Institute at 2500m a.s.l. These two systems are controlled by a computer at the Institute. Four systems (X-band) are installed in avalanche tracks at the Lukmanier Pass to monitor flow heights and slope-perpendicular avalanche speed profiles. The two sledge-mounted systems are used to measure the effect of trees and topography on snow stratification.

PRINCIPLE OF OPERATION AND DATA ANALYSES

The FMCW radar measures electrical distances between the radar and specular reflecting interfaces within the snowpack, the soil-snow and the soil-air interface. Electromagnetic radiation from the transmitting antenna (Figure 1) is beamed vertically at the snow pack either from above the snow cover (sledge-mounted systems) or from below the ground surface (buried systems). A triangular-modulation oscillator (sweep period $P=26.4\text{ms}$) sweeps the frequency of the microwave source as a linear function of time between the band limits (3.6 - 8GHz, 8 - 12.4GHz, 13.6 - 18GHz, bandwidth $B = 4.4\text{GHz}$). The second antenna receives the reflected radiation. The electrical distance, from

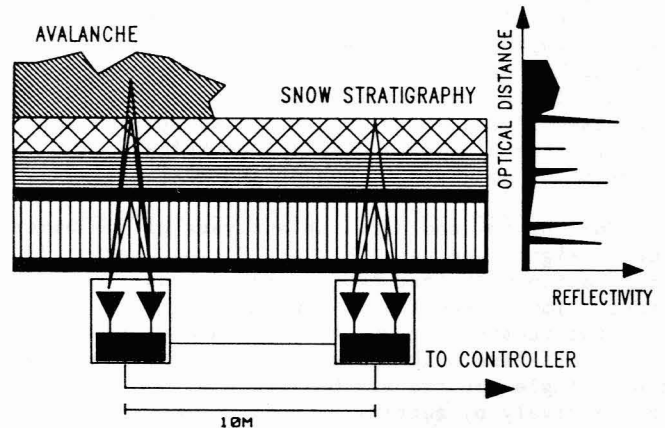


Figure 1. Principle of FMCW radar operation.

antenna to target and back, determines the difference in frequency between the signal transmitted, and that received at any instant. This frequency difference df determined by mixing the actual transmitting frequency with the receiver's frequency is related to electrical distance by the equation,

$$l = df \cdot P \cdot c / 4 \cdot B \quad (1)$$

where c denotes the speed of light. For the SFISAR systems, the conversion factor amounts to

$$df/l = 2172\text{Hz/m} \quad (2)$$

To convert electrical depth l to geometrical depth d , the following relationship proved reliable,

$$d = l / (1 + 0.771(\text{snowdens}/\text{icedens})) \quad (3)$$

where snowdens and icedens are the densities of

snow and ice. Frequency difference df is determined from the Fourier spectra of the radar's mixer output. For uniform windowing in the FFT (Fast Fourier Transform) algorithm, the -3db linewidth in units of distance in air is

$$\begin{aligned} LW(-3db) &= 0.44 * c / 4 * B & (4) \\ LW(-3db) &= 1.62 \text{cm} \text{ (35.2Hz)} \end{aligned}$$

The amplitude of the first sidelobe of the $\sin(f)/f$ spectral line envelope is only 13 db down from the main lobe amplitude. As a consequence of this, weak reflections may be masked by nearby strongly reflecting interfaces. Interferences of strong sidelobes with weak mainlobes originating from nearby strong and weak reflections may cause ambiguities in the interpretation of spectra. To remedy the problem the spectra should be deconvoluted using the theoretical line shape, but computing time to perform the deconvolution would be enormous. To decrease ambiguity we convolute the spectra with the theoretical envelope of the lobe amplitudes of a single line and subtract the convoluted spectra from the original one. Peaks remaining in the difference spectra are considered to be physically relevant. For a given microwave frequency, constructive and destructive interference between signals of different interfaces will occur. Fortunately the occurrence of this type of interference is significantly reduced by the 1/3 octave microwave frequency sweep. Significant interference occurs only for interface layers which are separated by less than one wavelength. A more complete technical description is given in Gubler and Hiller (1984).

For the on- and off-line analyses of the mixer output signal, we use a Hewlett Packard series 300 workstation with fast A/D and FFT boards. The codes allow automatic on-line measurements with two radars at given times each day, as well as for off-line high speed analyses from magnetic tape. Single spectra may be interpreted interactively by setting markers to spectral lines and either introducing measured or estimated layer densities to determine geometrical distances, or introducing geometrical distances to calculate waterequivalences. These types of analyses allow for a direct comparison of radar profiles to conventional ramhardness and morphological profiles.

Codes for automatic spectral line recognition are used to analyse large time series of spectra. Examples shown in this paper are: time series of spectra for seasonal snow covers, series showing avalanche flow over a radar, and series visualizing areal variation of the stratigraphy of natural snow covers.

FIELD TESTS

To investigate system performance under field conditions, different types of test measurements have been performed. Some of these experiments will be described here, and additional information is given in Gubler and Hiller (1984).

From the radar equation we may learn that the microwave return from a plane target decreases in

proportion to the inverse of the radar-to-target distance squared. The system built at SFISAR equalizes radar return signals from targets between 0.5 and 7m in medium density snow. Therefore relative amplitudes within a spectrum will depend on the distance between radar and snow. This dependence is clearly shown in Figure 2. The example shows that best overall contrast is achieved for a radar to snow distance of about .5m. The weakly structured middle parts of the spectra correspond to a heavy storm in January, 1986. It can also be seen from this series of spectra that the apparent resolution increases with decreasing radar-to-snow distance because of the decreasing footprint diameter (footprint is the area covered by the radar beam). Figure 2 shows an enhanced representation of the spectra as described earlier. Only significant peaks are shown. Nevertheless ambiguity remains for the weakly structured middle parts of the spectra.

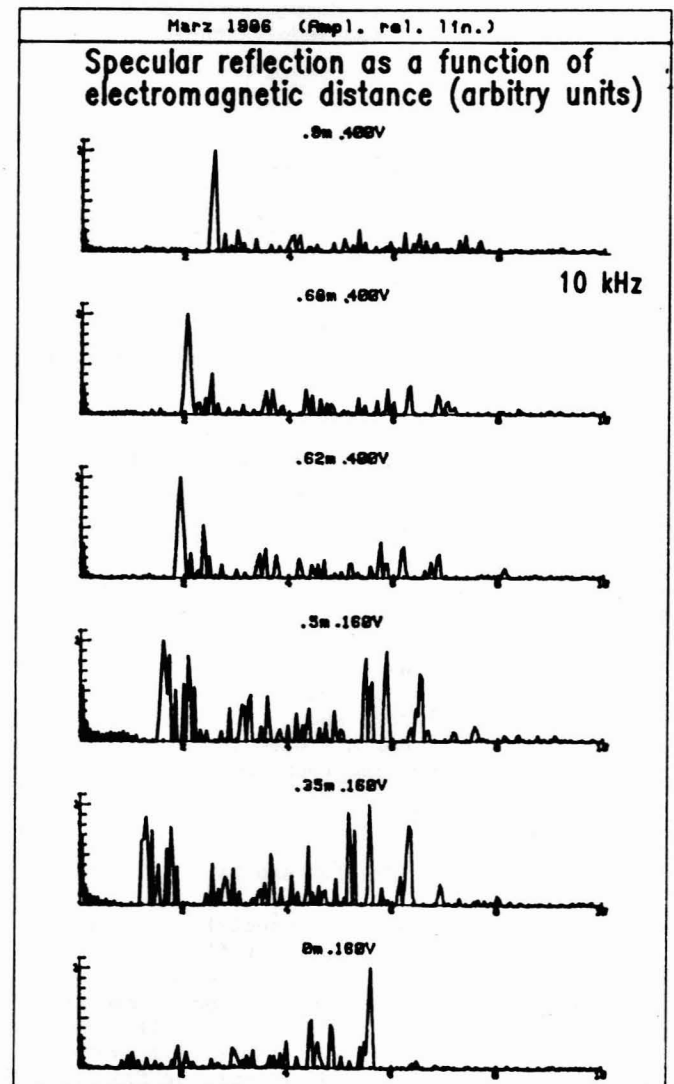


Figure 2. Enhanced spectra measured as a function of distance between radar and snow. The actual separation is given in the title of each spectrum.

For almost all spectra shown in this report, the frequency difference between calculated points (40Hz) is chosen to be about equal to the theoretical -3db width of a single frequency spectral line (35Hz). The first line contour minimum is at 80Hz, the first-order side lobe maximum is 120Hz apart from the central lobe peak. Analyses of real spectra at different resolutions have shown that this is a good compromise between increasing computing time for increasing point density and possible information loss at decreasing point density. These specifications also allow a high time resolution of one spectrum measured every 26ms.

In Figure 3 spectra of two radars looking from above into the snowcover and working at different frequencies (8-12.4GHz, 13.6-18GHz) are compared with the spectra of a third radar also working at the lower frequency but looking from below the snow cover. The radars were about 15m apart. The main features of the stratification can be recognized in

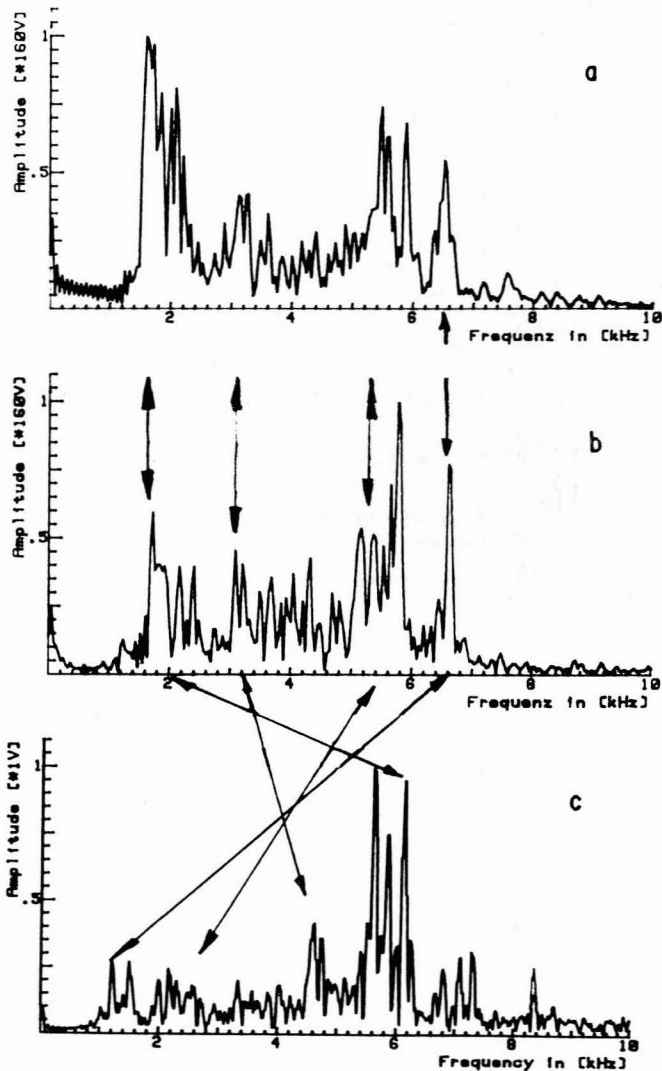


Figure 3. Comparison of spectra taken 11 on March 1986 from above the snow cover at different microwave frequencies a) 8-12.4GHz, b) 13.6-18GHz and c) from below the snow cover at the lower frequency with "mirroring" caused by corner reflectors.

all spectra, whereas the fine structure depends on frequency dependent interferences as well as on local variations of the layering and differences in viewing angle and footprint. For the buried radar, which is one of the study plot radars, small corner reflectors have been mounted at a height of about 4m above ground. These reflectors allow an approximate measurement of local waterequivalence without the need of an independent geometrical snow height measurement. The geometrical distance is given by the known height of the reflectors. For waterequivalence above 100mm this method produces very useful results. The disadvantage of these reflectors can clearly be seen from Figure 3c. Interferences between the strong corner reflector signals and strong signals originating from near-surface targets led to "mirror" peaks above 6.5kHz.

Volume scattering in dry snow for cm wavelengths is very low. The radars measure specular reflections from interface layers.

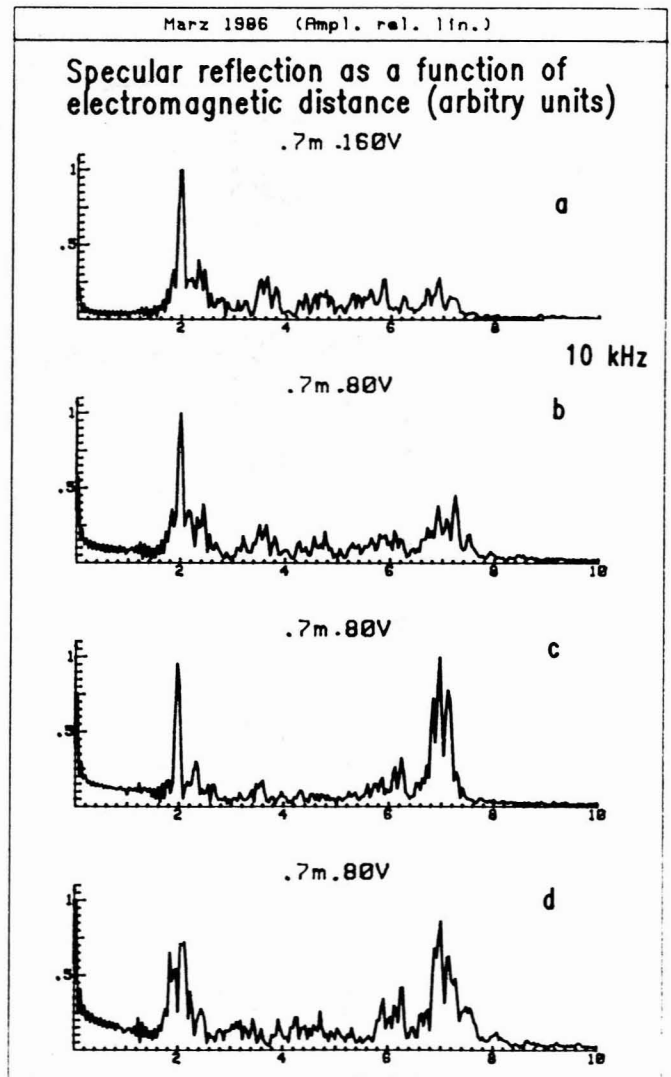
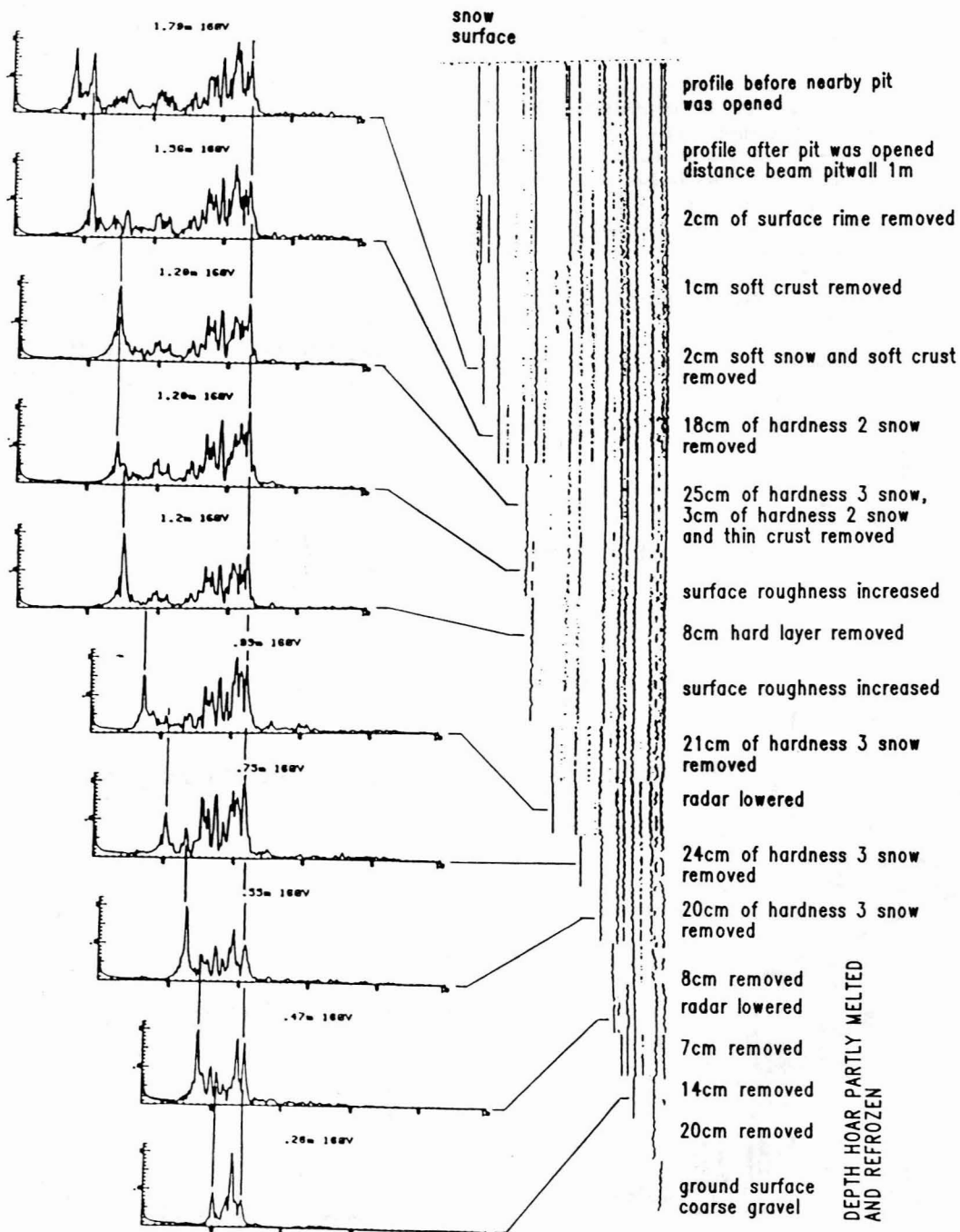


Figure 4. Series of spectra showing the effect of non slope-perpendicular incidence of the radar beam. a) normal incidence, b-d) incidence 10° from normal at 3 horizontal directions.

Measuring specular reflections with a system having the receiving antenna close to the transmitting antenna requires that the radar beam is perpendicular to the reflecting surface. Layer interfaces in a natural snow cover are never exactly flat and parallel. The effects of deviations of beam directions from normal incidence by 10° in different horizontal directions are shown in Figure 4. Obviously, snow surface and ground surface are not in parallel for the case shown. The

finite antenna resolution (7°) permits some deviation from perpendicular illumination at the cost of resolution. At L-band frequencies, where multioctave antenna having a very low spatial resolution have to be used, depth resolution is poor. For these cases we use plastic lenses to decrease the footprint and increase depth resolution, with good success.



radar reflection as a function of snow depth (arb.units) electromagnetic profile

Figure 5. Selected spectra and series of electromagnetic profiles of an experiment where the snow cover was removed layer by layer.

In the experiment shown in Figure 5, the snowcover was removed layer by layer. Radar profiles were taken at each stage. The electromagnetic stratifications, determined by using the code that automatically searches for significant spectral lines in consecutive spectra, are plotted together with a selected number of individual spectra. Some interesting effects can be seen from this series. Removing the thin very rough and low density surface hoar layer on top of the thin crust made this crust finally visible. The surface hoar performed an impedance match between the crust and air, and for this reason decreased the reflectivity of the crust. In the original spectra, not shown here, the hoar-crust combination can just be seen. In many cases the interfaces recognized by the radar are in perfect agreement with the mechanical interfaces found in the pit. In some cases of thin crusts, the radar did not resolve the upper and lower boundary of the crust, showing only a weak signal corresponding to one of the boundaries. Interference effects discussed earlier can occasionally mask thin crusts. Effects of interference and footprint diameter can be seen by comparing the shapes of the spectra for the

layers near the ground throughout the experiment. These layers consisted of partially melted and refrozen coarse-grained depth hoar. The experiment shows that a rough surface has a significantly reduced reflectivity.

In Figure 6 an electromagnetic profile is compared to the corresponding ram and morphological profiles.

Additional experiments have been done in dry snow to check validity of Equation 3 for a wide range of densities, snow stratifications and waterequivalences. The results support Equation 3 within a few percent for shallow snow covers (The problem of geometrical measurement is explained in Gubler and Hiller, 1984) and within 1% for waterequivalences above 300mm.

Experiments to measure mean snow wetness using a single radar or a combination of an L-band and an X-band radar were also performed. We found that absorption, reflection at water-saturated layers and basic resolution of the radars limit quantitative measurements severely. But the radars allow important insights into the vertical distribution of meltwater during the initial stage of melting of a seasonal snow cover.

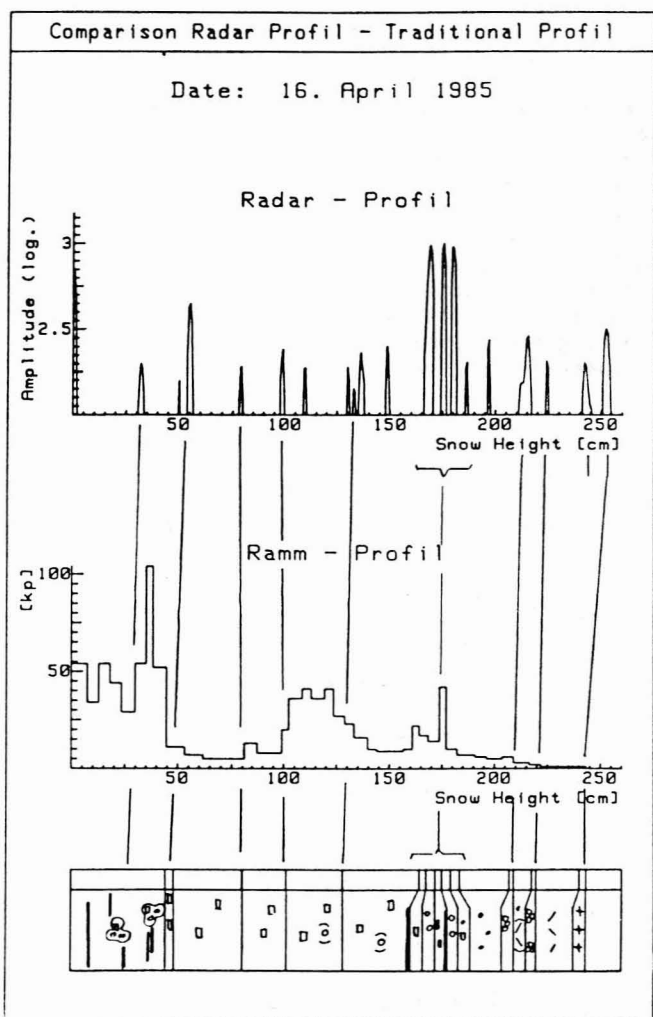


Figure 6. Comparison of a late winter radar spectra with the corresponding traditional snow and ram profiles. To enhance the spectra, a logarithmic power scale with a lower cutoff at the spectral noise floor has been chosen. Snow pit and radar were about 30m apart.

SELECTED APPLICATIONS AND RESULTS

We will discuss selected results of four applications of FMCW radar at SFISAR: 1) localized monitoring of the development of stratigraphy and waterequivalence during the winter season, 2) damming of water at interface layers during the initial springtime melt phase, 3) areal variations of snow stratigraphy, and 4) localized flow depth measurements in dense flow avalanches.

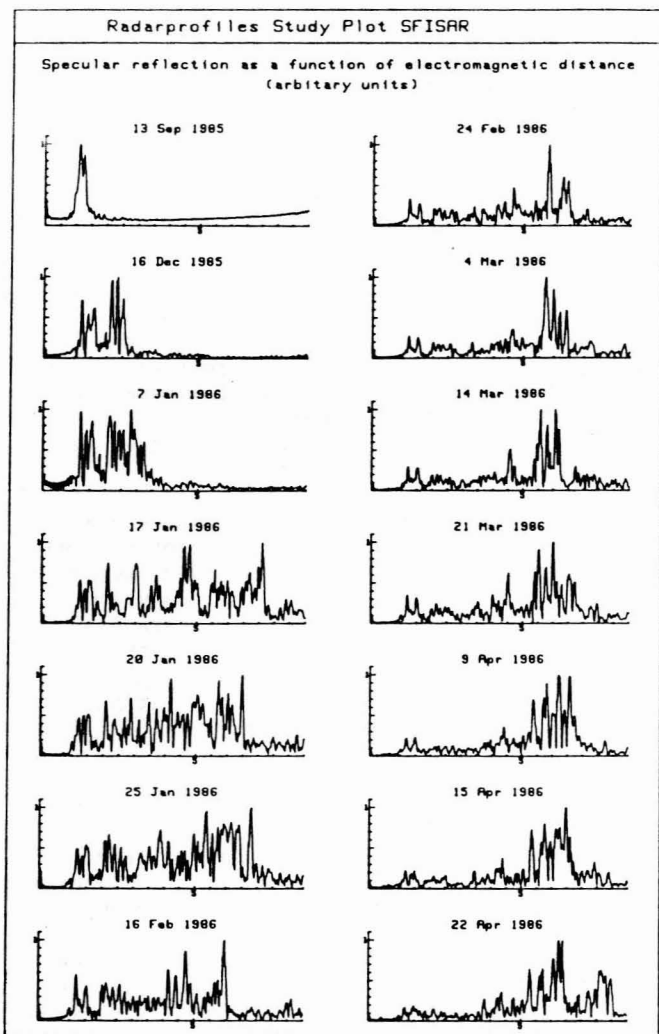
MONITORING OF SNOW STRATIGRAPHY

Waterequivalence and stratigraphy have been monitored in the SFISAR study plot at Weissfluhjoch since 1982 using FMCW radar. A selected number of typical spectra of winter 1985/86 are shown in Figure 7a. The bitmap presentation of the electromagnetic profiles is given in Figure 7b. To improve this type of presentation at least two measurements per day will be made in the future. The settling curves in Figure 7b allow a simple calculation of the increase of mean densities with time,

$$\text{findens} = \text{initdens} / (r - (1-r) * (n-1) * \text{initdens} / \text{icedens})$$

$$r = l_{\text{final}} / l_{\text{init}} \quad (5)$$

where initdens and findens denote initial and final mean densities, l_{init} and l_{final} , initial and final layer thickness, and n the index of refraction of ice (1.775). For the example in Figure 7b density increased from an estimated 190kg/m^3 immediately after the storm to 430kg/m^3 120 days later. These numbers are in good agreement with corresponding field data. Three selected spectra of Jan. 7/17/20 also show the fast increase of snow height followed by significant settling. Often settling can be



monitored during the storm, as an important indicator for increasing strength and stability. Because these radars can be placed within release zones without being damaged by avalanches, they provide an important tool to monitor snow accumulation, settling and avalanche releases in potential fracture zones.

MELT WATER PERCOLATION

Damming of meltwater at crusts or layer interfaces within the snow cover may lead to thin slush layers of very low strength responsible for wet snow slab releases. Buried X-band FMCW radars permit monitoring the initial phase of penetration of surface meltwater into the snow cover, damming of meltwater, and increasing wetness within layers. Several examples are shown in Figure 8. During the initial stage of melt of a seasonal snow cover, meltwater seems to percolate along preferred channels, even in snow below freezing, and is often dammed by crusts. Increasing liquid content at interfaces causes a significant jump of the index of refraction at these dry-wet interfaces. This results in a high reflectivity of the interface, causing a significant peak in the spectrum. If the liquid content within a layer reaches a few percent by volume, microwave absorption at X-band frequencies increases drastically. Penetration depth decreases from several hundred wavelengths in dry snow to a few wave lengths in wet snow, masking anything within or behind the wet layer. Figures 8a-e show meltwater damming during spring 83/84/85 at the SFISAR study plot and on a nearby northeast facing slope (Gems-luecke). Indexes for surface meltwater production, for the prevailing type of temperature profile and the amount of water reaching the ground (measured by a nearby lysimeter) are given for the different years.

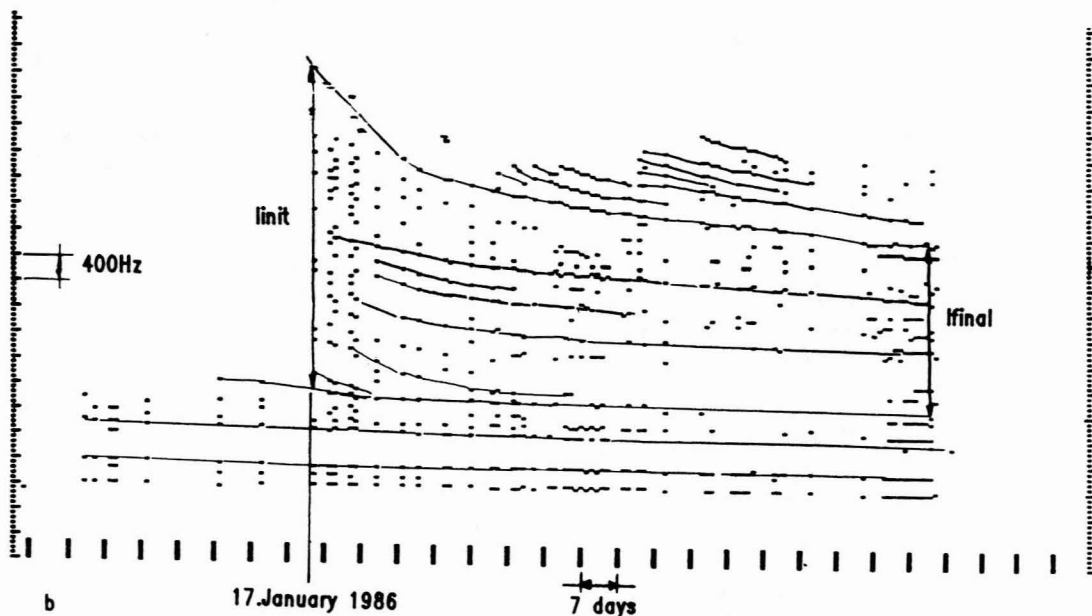


Figure 7. a) Selected spectra from the SFISAR study plot of winter 85/86 (buried system). b) Corresponding time series of electromagnetic profiles.

Normally surface melting starts in March. Often meltwater is dammed for several weeks. In spring '83 meltwater reaching the bottom of the snowpack on the slope was delayed by about 3 weeks compared to the study plot. The meltwater was routed downslope along an interface or crust. In spring '84 there was almost no delay. In '85 even though meltwater reached the bottom by the end of May, there remained significant damming at an interface about 40cm above ground for about 50 days. In Figure 8f selected spectra from spring '86 are given. Again surface melting started in late March. Some damming at two interfaces can be seen in the spectrum of 2 April. Noticeable settling occurred during April. Between the 1 May and 2 May,

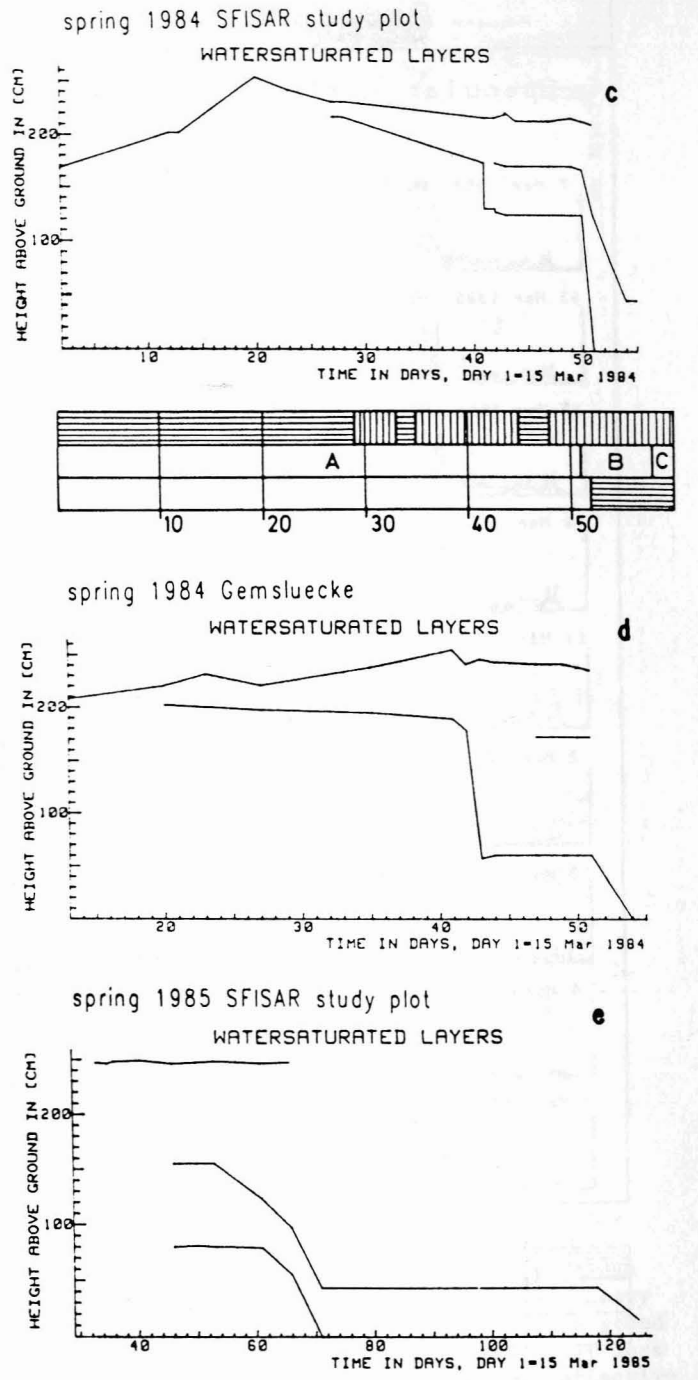
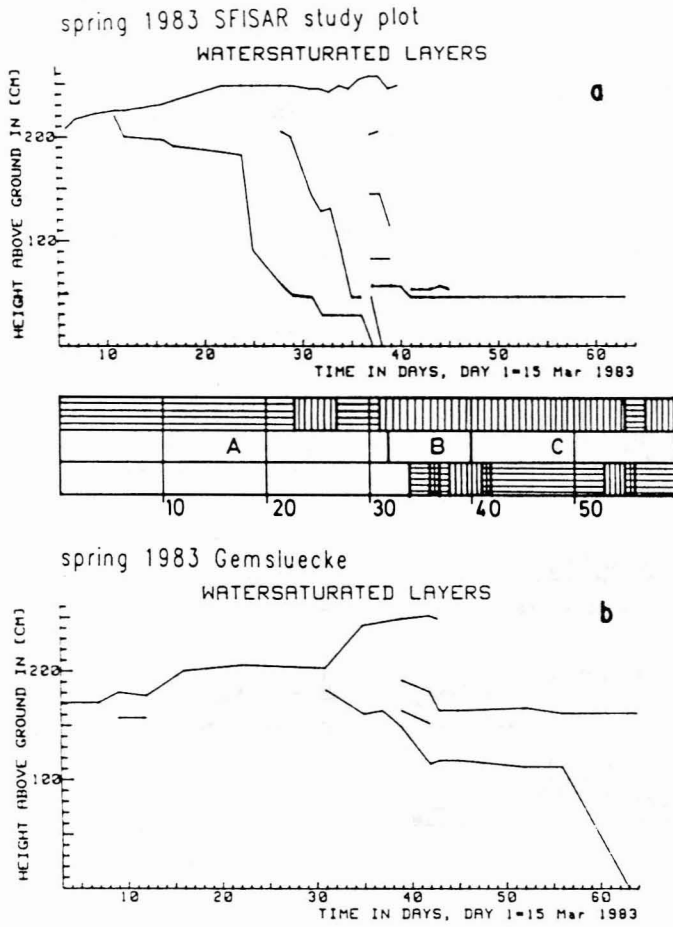


Figure 8a-e. Damming and percolation of meltwater in the SFISAR study plot and a nearby northeast facing slope for springs 83,84,85. The uppermost line in a-e) indicates total snow height, the lower lines water saturated layers.

Specular reflection as a function of electromagnetic distance
(arbitrary units)

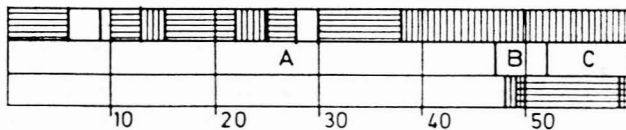
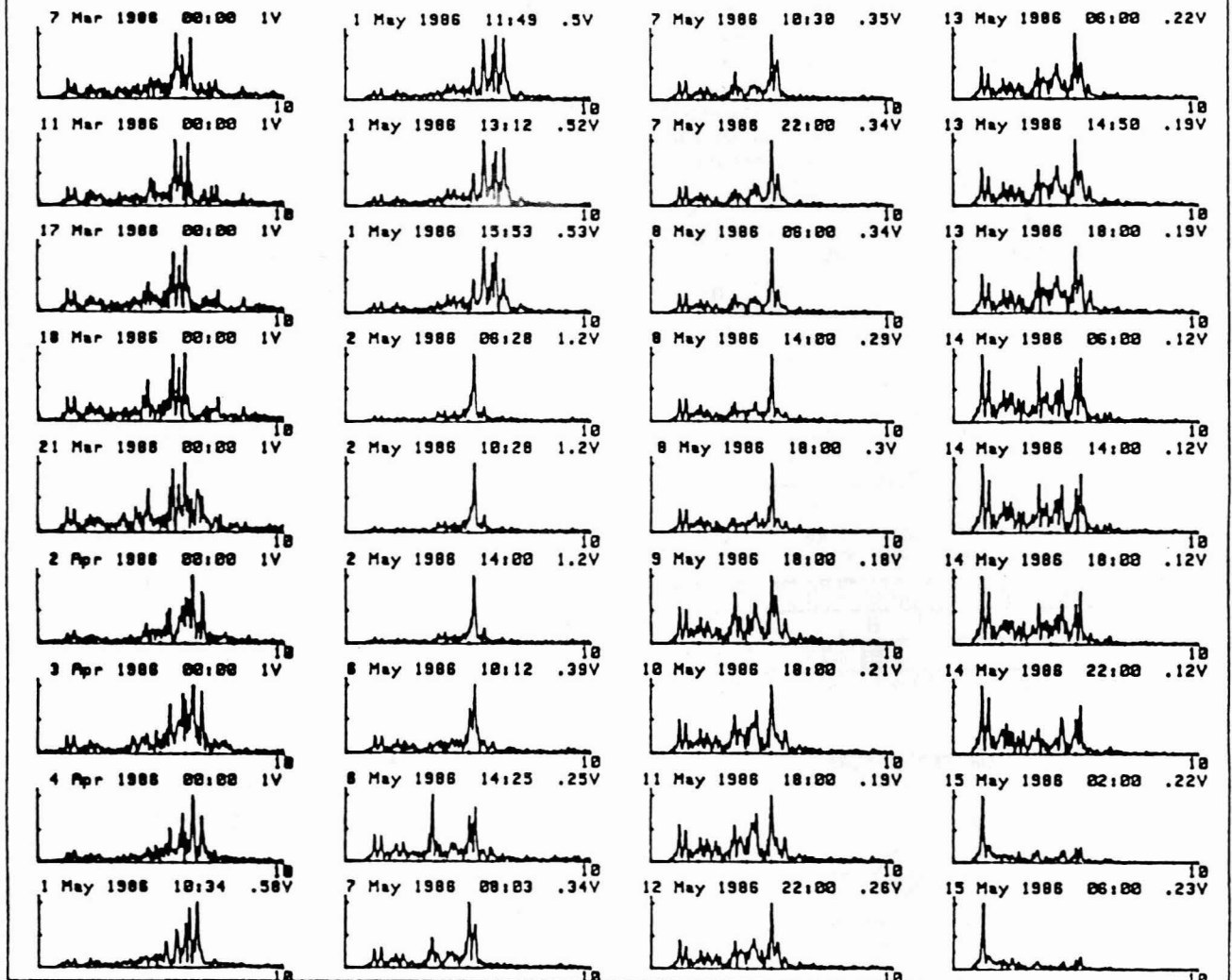


Figure 8f. Selected spectra of spring '86.

meltwater penetrated and was dammed at a lower interface. Some meltwater reached the bottom of the pack through channels, but the layers below the damming interface remained mainly dry. On 6 May water concentrated for a short time at a lower level. Until 14 May not much melting occurred. Some of the water seems to be refrozen or to be routed through the now existing channel system to the ground, leaving the main part of the pack still almost dry. But on the 15 May, after the onset of significant meltwater production at the surface, the dammed meltwater broke through, homogeneously wetting the rest of the snow pack.

Several conclusions can be drawn from these observations: Meltwater may penetrate cold snow in

preferred channels. Damming of meltwater may delay homogeneous wetting of underlying layers for long periods of time. This effect is even more pronounced if meltwater flows downslope along impermeable layers. Meltwater originating from the surface may reach the ground before the snow cover is isothermal.

STRATIGRAPHY PROFILING

Local variability of the stratigraphy significantly effects slab releases. Forests are known as an effective protection against slab releases. But today, unfortunately, air pollution seems to severely damage protective forests. For

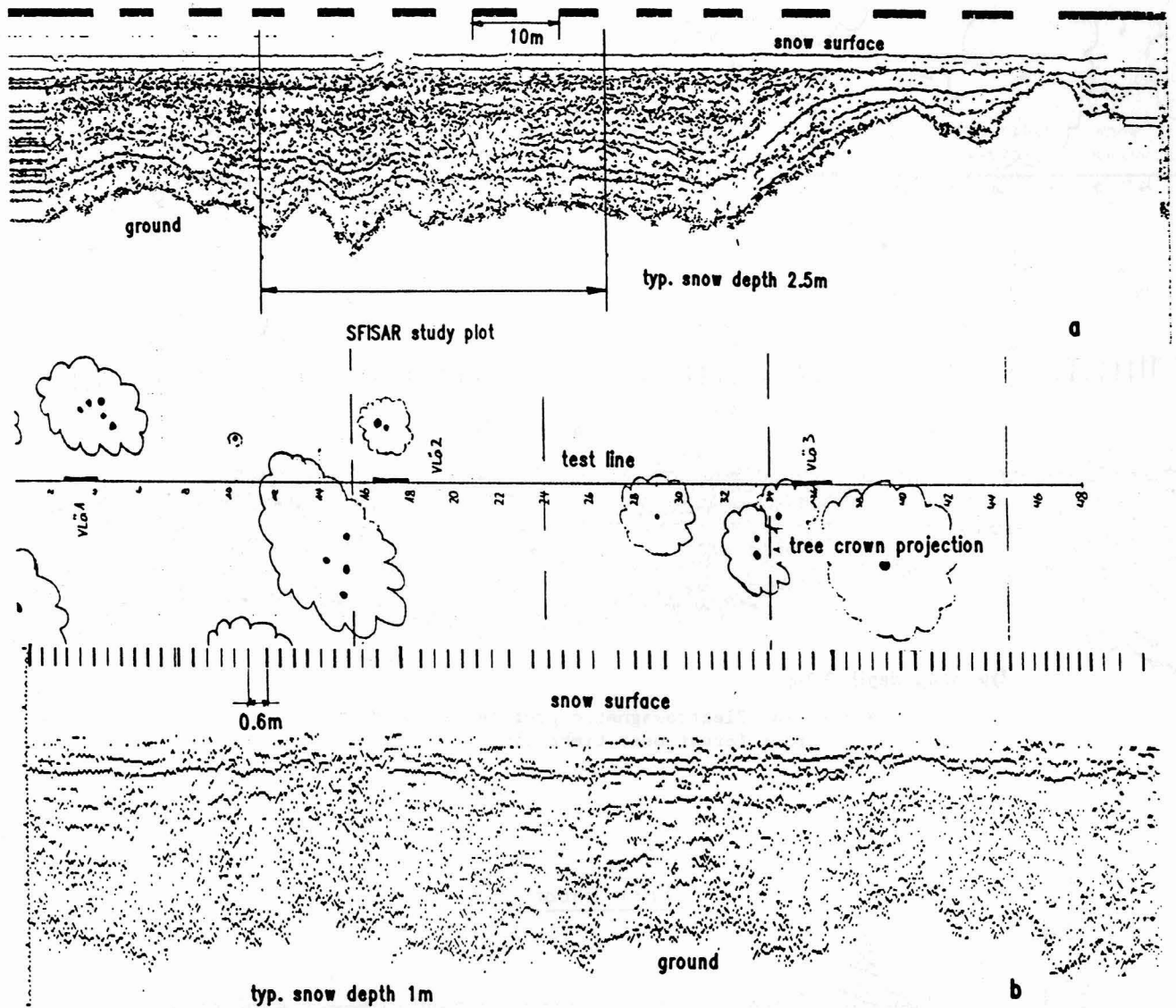


Figure 9a,b. Examples of electromagnetic profiles taken along test lines. a) SFISAR study plot, b) larch forest at timberline.

this reason we have to define minimum specifications for protective forests to give foresters a tool for their decisions on where and how to start additional protective measures. In forests, the trees influence the microclimate, the tree crowns intercept snow, and delayed snow falls occur from tree branches. These facts change the stratigraphy in the vicinity of a tree compared to a free-field profile. The sledge-mounted radar is used to measure the extent of these influences. In Figure 9, three examples are given. Figure 9a shows a typical free-field situation at the SFISAR study plot. Total snow height varies significantly along the test line as the result of strong drifting in the open. Figure 9b shows the stratigraphy in a typical larch stand at timberline. The influence of the larch crown on the stratigraphy is small. The large roughness of the ground surface seems to affect stratigraphy more effectively. A larger amount of snow is necessary in these types of forest, compared to the free-field situation (meadows), to smooth the ground allowing for a more continuous layering. In the free-field, strong snow

drifting may smooth the surface with less snow available. But snow drifting is decreased by forests. The larch stand shown is typical for a forest where slabs may release during very heavy storms. Figure 9c shows a more dense spruce stand at the same location. There is significantly less snow, interception seems to be much more effective and very little layering can be found at all. This type of forest will normally prevent slab releases.

MEASUREMENT OF AVALANCHE FLOW HEIGHT

The problem of measuring flow heights and slope perpendicular flow speed profiles in dense flow avalanches was the motivation for developing FMCW radar at SFISAR. Four radars are buried in avalanche tracks at our avalanche study site on the Lukmanier Pass. An example of an avalanche flowing over two radars, which are buried at a slope distance of 16m is shown in Figure 10. The pictures show the avalanche flowing over the static part of the snowcover. A rock barrier above the upper radar

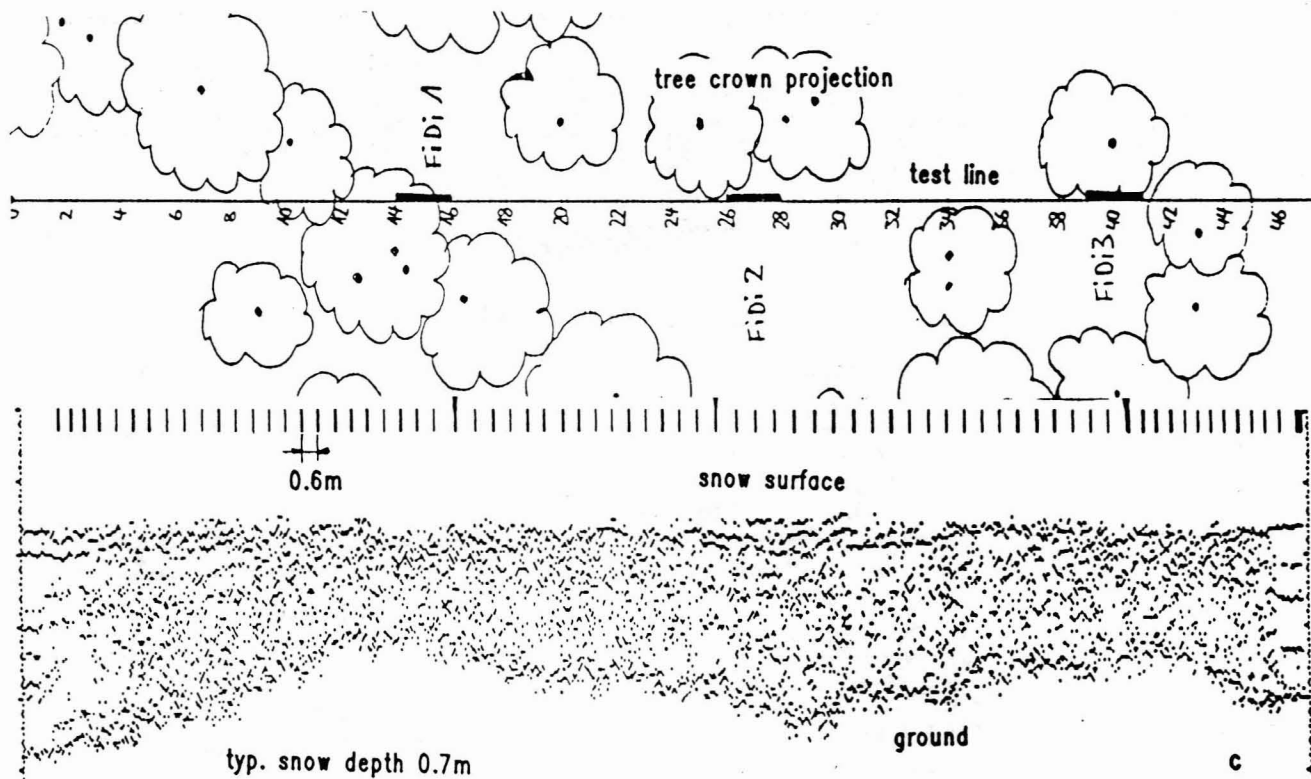


Figure 9c. Electromagnetic profile measured in a spruce forest near timberline.

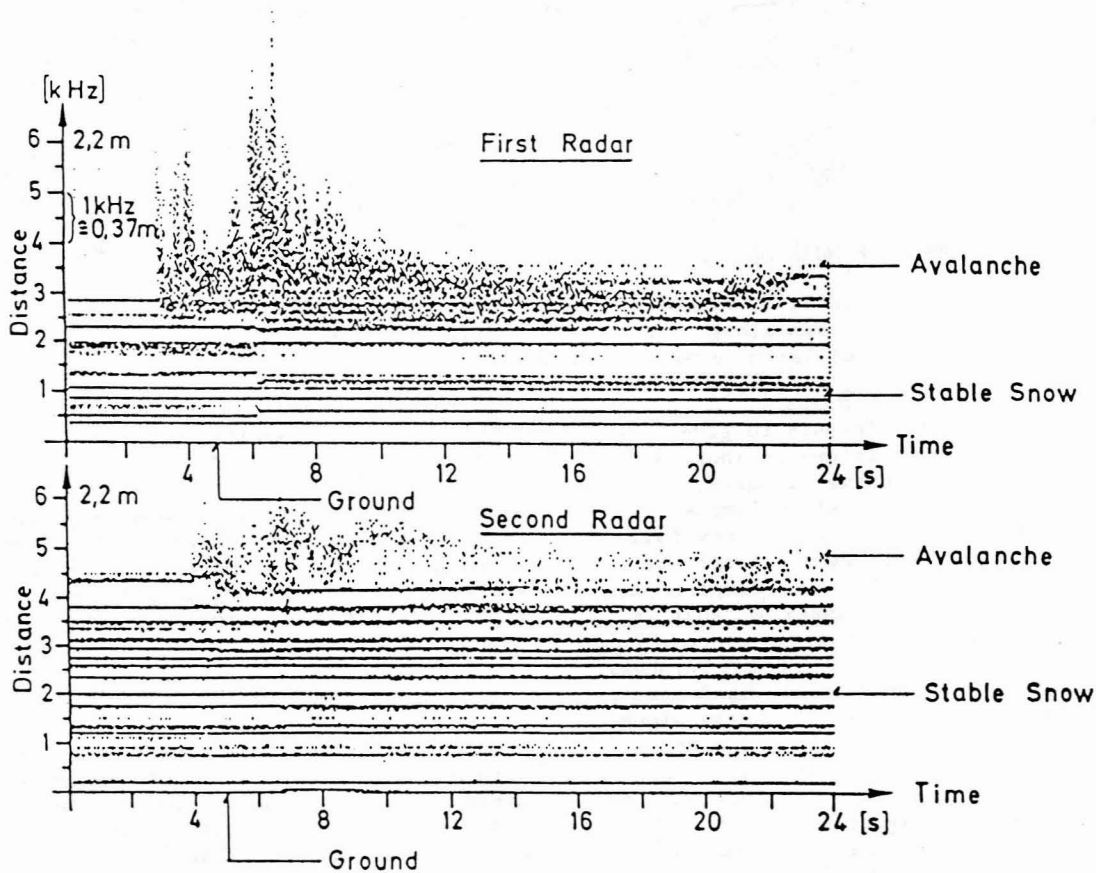


Figure 10. Electromagnetic, slope-perpendicular profile of a dense flow avalanche measured with two radars at a downslope distance of 16m.

ejects some snow in the air as can be seen on the top plot.

CONCLUSIONS

In our opinion, FMCW radar is a very powerful tool for many different qualitative and quantitative investigations of the snow cover and avalanches. Because the instrument can be buried in the ground, it is well protected from the harsh environmental conditions. The technique is fairly simple and reliability proved to be very high. Many operational applications can be envisioned: Monitoring of stratigraphy, loading, settling, waterpercolation, slab releases in avalanche release zones; monitoring of avalanche flows in tracks for local warning systems; monitoring of waterequivalence and meltwater percolation for hydrological purposes.

ACKNOWLEDGMENT

We would like to thank M.Hiller and G.Klausegger for their continuing help to maintain the systems and R.A. Schmidt (USDA, Fort Collins, USA) for his careful review of the manuscript.

REFERENCES

- Ellerbruch, D.A. and H.S.Boyne (1980). Snow stratigraphy and waterequivalence measured with active microwave system. Symp. Snow in Motion. J. of Glaciology 26:225-233.
- Gubler, H. and M.Hiller (1984). The use of microwave radar in snow and avalanche research. Cold Region Science and Technology 9:109-119.
- Gubler H.,M.Hiller and R.A.Schmidt (1985). FMCW radar for snow cover investigations. Internal Report no 627 SFISAR.
- Schmidt, R.A., H.Gubler and M.Hiller (1984). Swiss improvements of the FMCW radar for snow measurements. Proceedings of the 52nd Annual Western Snow Conference, April 1984, at Ketchem, Idaho.